Charge Distribution in Arylhydrazine-Centered Mixed Valence Compounds with Smaller Bridges (Five to Nine Bonds between Closest Nitrogens)

Stephen F. Nelsen* and Kevin P. Schultz

Department of Chemistry, University of Wisconsin, 1101 University Avenue, Madison, Wisconsin 53706-1396

Received: December 3, 2008; Revised Manuscript Received: February 9, 2009

Charge distribution in six aromatic-bridged, aryldialkylhydrazine-centered mixed valence radical cations is discussed through consideration of their optical spectra. The compounds considered have two 2-phenyl-2,3-diazabicyclo-[2.2.2]octane-3-yl (**HyPh**) charge-bearing units linked by a 1,4-phenylene bridge and its *p*-methoxyphenyl (**HyAn**) analogue, as well as the (**HyPh**)$_2$-substituted 1,4-naphthalene, 2,6-naphthalene, 9,10-anthracene, and 4,4′-biphenyl compounds in methylene chloride and acetonitrile. Consideration of band shape and position leads us to assign the 1,4-phenylene- and 2,6-naphthalene-bridged compounds as charge-delocalized (class III) in both solvents, but the 1,4-naphthalene-bridged one lies closer to the borderline, and appears to be charge-localized (class II) in acetonitrile. The 4,4′-biphenyl-bridged compound is clearly class II in acetonitrile, and possibly also in methylene chloride. The lowest energy absorption band for the 9,10-anthracene-bridged compound is assigned as a bridge-to-**HyPh** band, and its charge distribution is not clear. Problems with the often-used relationship that the electronic coupling is half the transition energy for the lowest energy band of class III mixed valence compounds are discussed, as is interpretation of the vertical reorganization energy near the class II, class III borderline.

Introduction

The simplest mixed valence (MV) compounds have two charge-bearing units (CBUs, **M**) attached to a bridge (**B**) and are at an oxidation level where the charges on the CBUs might be different, so they are radical ions.[1−3] The concept was devised for transition metal coordination complexes that have one bivalent ligand bridging the metals, but this paper concerns all-organic examples with aryl bridges and arylhydrazine CBUs. We principally address here the question of whether the charge is mostly localized on one **M** group, so that a radical cation example would be usefully considered to be **M^0-B-M$^+$** (called a Robin−Day[1] class II system), or whether the charge is delocalized, so the **M** groups have equal fractional charges, and a more significant amount of the charge occurs on the bridge (class III). Charge delocalization occurs when the electronic coupling, H_{ab}, exceeds half of the reorganization energy, λ. Marcus−Hush energy diagrams illustrating these two classes of compounds appear as Scheme 1.

We initially became interested in all-organic hydrazine-centered MV compounds to test Hush's remarkably simple evaluation of both λ, equal or close to the band maximum transition energy, $\bar{\nu}_{max}$, and H_{ab}, given by eq 1 (in the form in which it is usually used),[3]

$$H_{ab} = 0.0206(\bar{\nu}_{max}\Delta\bar{\nu}_{1/2}\varepsilon_{max})^{1/2}/d_{ab} \quad (1)$$

from the charge-transfer band absorption spectrum of class II compounds (for energies in cm^{-1} and the electron distance d_{ab} in Å; $\Delta\bar{\nu}_{1/2}$ is the full width at half-height, and ε_{max} is the extinction coefficient in M^{-1} cm^{-1}). For this purpose, we used **HytBu** (see Chart 1) as the **M** groups when aromatic bridges were employed, and measured electron-transfer rate constants using electron spin resistance (ESR).[4−10] These studies showed that the electron-transfer parameters calculated using Hush theory predict the electron-transfer rate constants remarkably well, and that agreement with experiment is improved by minor adjustments to Hush's method (including a refractive index correction to ε_{max} and changing the way d_{ab} is estimated). In subsequent work to be reported separately, we have examined larger bridges, which required increasing the rate constants from those obtained using **M** = **HytBu** to keep them in the range measurable by ESR, near 10^8 s^{-1}, at accessible temperatures. We have done so by employing aryl third substitutents at nitrogen, **HyPh** or **HyAn**, which have been shown to substantially lower λ_v,[9,11] and also raise H_{ab} because there is less twisting at the CN bonds connecting the substituents to the bridge, so the rate constants are significantly larger than for **HytBu**-substituted examples. In contrast to nitro-centered radical anions[12−15] and dialkylamino-centered radical cations,[16,17] where the optical spectra of delocalized (class III) species show vibrational fine structure because the absorption bands are relatively narrow, the much-studied diarylamino-centered ones,

SCHEME 1: Marcus−Hush Diagrams Illustrating Class II and Class III Energy Curves

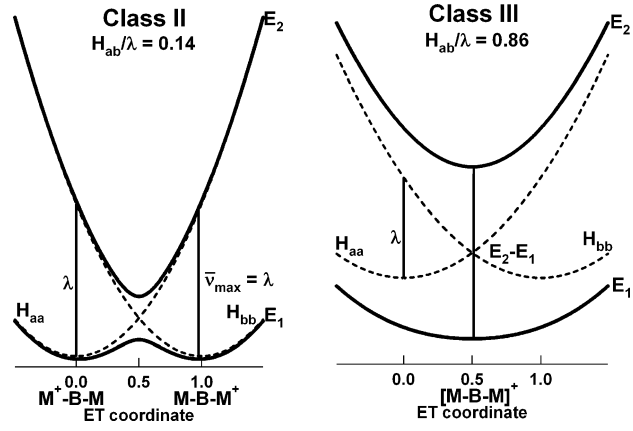

10.1021/jp810645q CCC: $40.75
Published on Web 04/08/2009

CHART 1: Charge-Bearing Units (M Groups) Considered Here

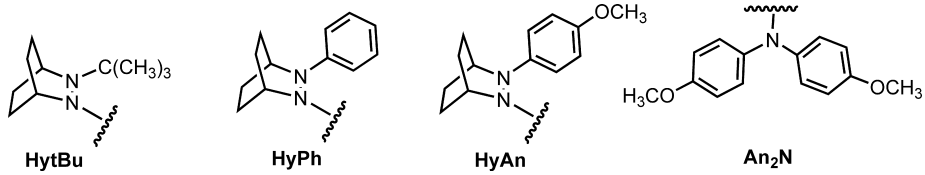

such as **An$_2$N**,[18−24] do not show a clear change in the optical spectrum when the charge delocalizes. Considerable discussion of whether or not delocalization has occurred for various examples has resulted. This work shows that **HyAr**-centered radical cations also do not show vibrational fine structure in their lowest energy absorption band when they are delocalized. Following literature precedent, the change in optical spectrum between the commonest polar and nonpolar solvents for such measurements on radical cations, MeCN (AN) and CH_2Cl_2 (MC), are considered here as possible criteria for determining whether charge is localized or delocalized. Comparison of the optical spectra in these two solvents emphasizes examining changes in transition energy, $\bar{\nu}_{max}$, and in bandwidth, because, according to the classical analysis that Hush introduced, there will be no absorption at lower energy than $2H_{ab}$, the minimum separation of upper and lower energy surfaces using the two-state model. When $2H_{ab}$ becomes a significant fraction of the MV band transition energy, this should lead to a noticeable cutoff of the ordinarily nearly Gaussian shape of the MV band on the low energy side, making the band asymmetrical, with low energy half-width smaller than high energy bandwidth and total bandwidth less than the Hush prediction of $(16RT\ln(2)\bar{\nu}_{max})^{1/2}$, which applies to class II compound absorption bands, using perfect parabolas for the diabatic surfaces.[19,25] This expectation of decreased bandwidth before charge delocalization occurs initially led to assignment of the smaller-bridged **An$_2$N**-centered compounds as class II compounds, but it is now realized that class III compounds with larger π system **M** groups would have similar shapes to what was expected for class II with a cutoff, because large line widths broaden out the vibrational fine structure. Although Nelsen, Zink, and co-workers have pointed it out,[14,26,27] it is less often accepted that a single two-state model should not be directly applied to class III mixed valence compound optical spectra of the type considered here to obtain H_{ab} using the convenient $H_{ab} = \bar{\nu}_{max}/2$ relationship. The narrow and intense low energy transitions that are observed and have traditionally been called the MV transition are not closely related to the MV transition of class II compounds. This occurs because class III compounds are symmetric, so a transition that involved only a single two-state splitting would be forbidden by symmetry and therefore weak. In other words, the energy gap labeled E_2-E_1 at the right side of Scheme 1 is $2H_{ab}$, but the energy of the narrow and intense optical transition of class III compounds that people have used to measure it does not correspond to $2H_{ab}$. These bands are well-known to be between MOs of different symmetry, so they cannot be the upper and lower energy surfaces related by a single electronic coupling that using $\bar{\nu}_{max}/2$ implies. However, the transition energy behaves as H_{ab} is expected to behave as the bridge size is increased, and it is not clear how large an error is introduced by equating $\bar{\nu}_{max}/2$ with H_{ab}.

The bridges discussed here are shown in Chart 2. Compounds are identified by the combination of acronyms for CBUs and bridges. As will be shown below, **HyAr**-centered cases having the smaller aromatic bridges are charge-delocalized.

CHART 2: Structures of the Bridges Discussed Here

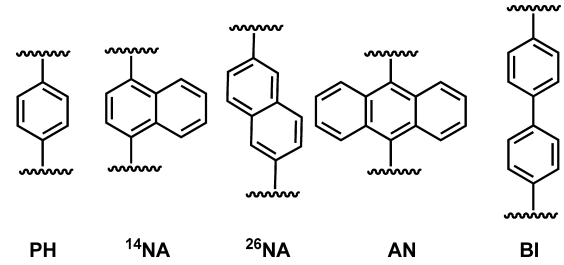

Results

As in previous work, the aryl bishydrazines were prepared by adding bis-lithio salts of the aromatic bridge, prepared from brominated aromatic compounds, to suitably substituted diazenium cations, as described in the Experimental Section. Although it is not important for this work, the **HyPh** groups actually used were pentadeuterated at the phenyl ring, to make them the same as those of the larger-bridged examples that will be discussed elsewhere, where deuteration was necessary to narrow their ESR spectra for rate constant determination.

Cyclic voltammograms were run in dry, nitrogen saturated methylene chloride in the presence of 0.1 M tetrabutylammonium perchlorate (TBAP) as the supporting electrolyte at a 100 mV/s scan rate. The working electrode was a 3 mm diameter platinum disk, the auxiliary electrode was a straight platinum wire, and the reference electrode was Ag/AgCl, but ferrocene ($FeCp_2$) or decamethylferrocene ($FeCp^*_2$) were used as internal standards, and potentials are reported versus the saturated calomel electrode, using $FeCp_2$ ($E^\circ = +0.395$ V) or $FeCp^*_2$ ($E^\circ = -0.110$ V). The electrochemical data are summarized in Table 1.

For the comproportionation equilibrium of a +1 charged MV compound, $[2+] + [0] \rightleftarrows 2[+]$, the comproportionation equilibrium constant K_{comp} can be obtained from the difference in oxidation potentials using $RT\ln K_{comp} = -nF(E^\circ_2 - E^\circ_1)$, where n is the number of electrons in the redox process, F is the Faraday constant (23.06 kcal mol^{-1}·V^{-1}), and R is 0.001 987 kcal mol^{-1} K^{-1}. If there were no interaction between the CBUs of a MV compound, K_{comp} would be 4, and the difference in first and second formal potentials, $E^\circ_2 - E^\circ_1$ would have the statistical value of 35.7mV. Qualitatively, a larger value of K_{comp} (and a large $\Delta E^\circ_2 - \Delta E^\circ_1$) indicates a greater interaction between the CBUs and a smaller K_{comp} would suggest a smaller interaction. Many groups have therefore used K_{comp} to estimate the electronic coupling element H_{ab} as described by Taube.[28] There have been more recent cautions about using this procedure, which ignores solvation differences caused by charge except for assuming that dielectric continuum theory correctly produces the solvent reorganization energy, and can lead to large errors.[8,29,30] We therefore will not try to use the data of Table 1 to estimate electronic couplings.

The optical spectra for compounds with the bridges shown in Chart 2 are shown below in Figures 1−6. The neutral compounds were oxidized with less than one equivalent of

TABLE 1: Summary of Cyclic Voltammetry Data (Units of mV) in Methylene Chloride at 100 mV/s [Potentials Reported versus SCE Using $FeCp_2$* as Internal Standard ($E^\circ = -110$ mV)]

cmpd	**(HyPh)$_2$PH**	**(HyAn)$_2$PH**	**(HyPh)$_2$^{14}NA**	**(HyPh)$_2$^{26}NA**	**(HyPh)$_2$^{910}AN**	**(HyPh)$_2$BI**[a]
bonds	5	5	5	7	5	9
$\Delta E_p^{FeCp_2*}$ [b]	120	115	115	130	90	
E°_1 [c]	260	225	340	400	190	445
ΔE^p_1 [d]	170	150	160	180	105	120
E°_2 [c]	595	540	520	575	*e*	594
ΔE_p^2 [d]	150	140	180	130	*e*	~135
$E^\circ_2 - E^\circ_1$	335	315	180	175	*e*	145

[a] $FeCp_2$ used as internal standard. [b] Difference between oxidation and reduction waves for decamethylferrocene. [c] $E^\circ = E_p^{ox} + E_p^{red}/2$. [d] $\Delta E_p = E_p^{ox} - E_p^{red}$. [e] First and second redox waves are overlapping.

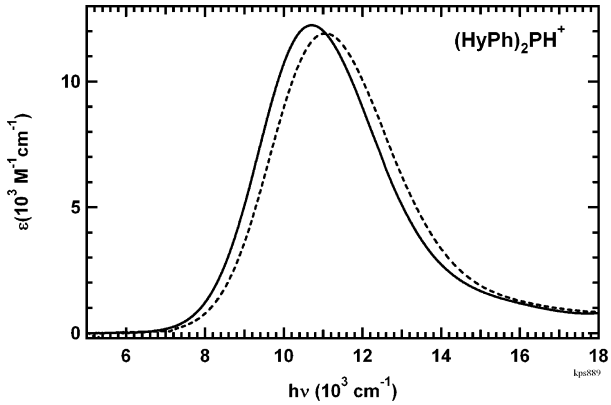

Figure 1. MV band of **(HyPh)$_2$PH**$^+$ in CH_2Cl_2 (solid) and CH_3CN (dotted).

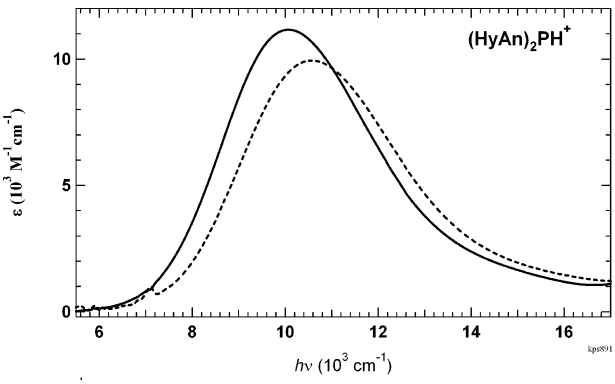

Figure 2. MV band of **(HyAn)$_2$PH**$^+$ in CH_2Cl_2 (solid) and CH_3CN (dotted).

oxidant, which ensures that almost only radical cation is present at equilibrium for compounds with as large E° differences as these (except **(HyPh)$_2$AN**, for which the oxidation waves overlap). A "solvent switch" was most often used to obtain the spectra in AN, by carrying out the oxidation in MC, carefully removing the silver reduction product, and blowing off the volatile MC while adding AN as described in the Experimental Section. This was done because the oxidation potential of the silver salt oxidant in AN was below that of the neutral compound. Figures 1 and 2 compare spectra in MC and AN, for the **PH**-bridged compounds. Figures 3 and 4 compare spectra in MC and AN for the isomeric **NA**-bridged compounds. Figure 5 compares the **HyPh**-centered with the previously studied **HytBu**-centered **AN**-bridged compound[31] in MC. Figure 6 compares the spectra for **(HyPh)$_2$BI**$^+$ in MC and AN.

Discussion

Optical band information from the literature for the **(HytBu)$_2$B**$^+$ compounds is summarized in Table 2. All of the

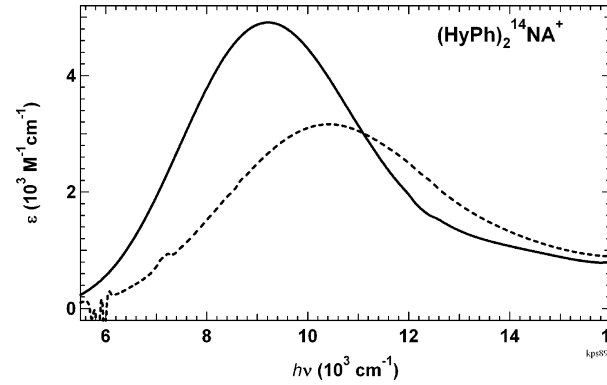

Figure 3. MV band of **(HyPh)$_2$^{14}NA**$^+$ in CH_2Cl_2 (solid) and CH_3CN (dotted).

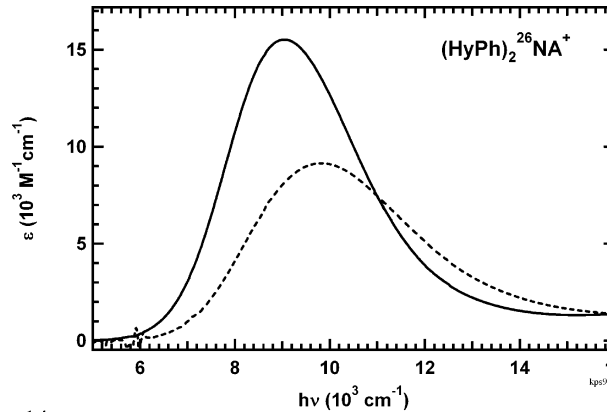

Figure 4. MV band of **(HyPh)$_2$^{26}NA**$^+$ in CH_2Cl_2 (solid) and CH_3CN (dotted).

HytBu-centered compounds of Table 2 are unquestionably localized; each showed evidence for slow electron transfer on the ESR time scale at low enough temperature.[10] Their $\Delta\bar{\nu}_{1/2}$ ratios are as expected all 1.00 or greater, consistent with Hush theory.[3] Their $\Delta\bar{\nu}_{max}$ differences ($\bar{\nu}_{max}$(AN) $-$ $\bar{\nu}_{max}$(MC)) are in the range 1800−2200 cm^{-1} for the compounds for which the lowest energy band is the class II MV band (the **AN**-bridged compound is an exception, see footnote *e*). Large sensitivity of $\Delta\bar{\nu}_{max}$ to solvent changes has always been used as a criterion for class II compounds, because for them $\Delta\bar{\nu}_{max} = \lambda$, and the solvent-dependent contribution to λ, λ_s, varies. Much smaller, but still detectable changes in the same direction are observed for strongly trapped class III compounds such as the bis(dimethyl-amino)-substituted *p*-phenylene diamine radical cation ($\Delta\bar{\nu}_{max}$ = 50 cm^{-1}) and its 4,4′-biphenyl analogue ($\Delta\bar{\nu}_{max}$ = 100 cm^{-1}).[16] Hush theory also predicts ε_{max} to increase in MC relative to AN for class II compounds, because $\bar{\nu}_{max}$ is smaller in MC, and the H_{ab} value is not expected to change significantly. The changes in ε_{max} (MC $-$ AN), which are more difficult to

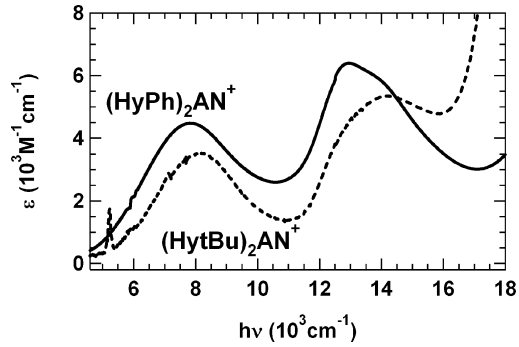

Figure 5. Comparison of optical spectra of **(HyPh)$_2$ AN**$^+$ (solid) and **(HytBu)$_2$AN**$^+$ (dotted) in CH_2Cl_2.

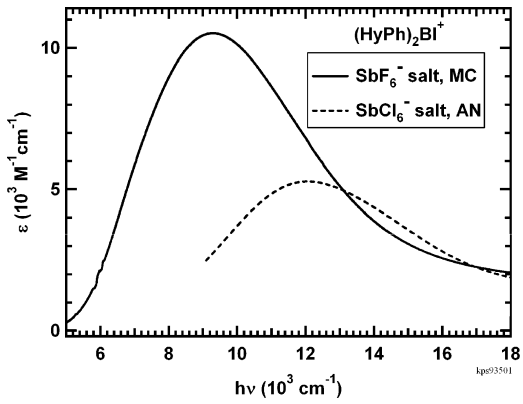

Figure 6. MV band of **(HyPh)$_2$BI**$^+$ in CH_2Cl_2 (solid) and CH_3CN (dotted).

TABLE 2: Comparison of Optical Spectra for (HytBu)$_2$B$^+$ Mixed Valence Compounds ($\bar{\nu}_{max}$, $\Delta\bar{\nu}_{1/2}$, and $\Delta\bar{\nu}_{max}$ Are in Units of 10^3 cm^{-1}, and ε_{max} Is in Units of 10^3 M^{-1} cm^{-1})

		in CH_2Cl_2 (MC)			in MeCN (AN)				
B	n^a	$\bar{\nu}_{max}$ (ε_{max})	$\Delta\bar{\nu}_{1/2}$	$\Delta\bar{\nu}_{1/2}$ ratio^b	$\bar{\nu}_{max}$ (ε_{max})	$\Delta\bar{\nu}_{1/2}$	$\Delta\bar{\nu}_{1/2}$ ratio^b	$\Delta\bar{\nu}_{max}{}^c$	$\Delta\varepsilon_{max}{}^d$
PH	5	10.80 (5.50)	5.70	1.14	13.00 (3.80)	6.46	1.18	2.20	1.70
^{26}NA	7	11.50 (3.70)	6.05	1.18	13.30 (3.30)	5.68	1.03	1.80	0.40
^{14}NA	5	10.84 (4.16)	5.77	1.16	12.68 (2.13)	5.40	1.00	1.84	2.03
AN	5	7.70 (2.12)^e			9.00 (1.40)^e			1.30^e	0.72^e
BI	9	13.00 (2.65)	6.27	1.15	15.20 (2.60)	6.09	1.03	2.20	0.05

^{a} Bonds connecting closest nitrogen atoms. ^{b} Ratio of the observed $\Delta\bar{\nu}_{1/2}$ to the Hush minimum value of $(16RT\ln(2)\bar{\nu}_{max})^{1/2}$ for a class II compound using parabolic diabatic surfaces. ^{c} $\bar{\nu}_{max}$(AN) − $\bar{\nu}_{max}$(MC). ^{d} ε_{max}(MC) − ε_{max}(AN). ^{e} Assigned to bridge oxidation, anthracene to **Hy**$^+$ electron transfer, so these bands are not directly comparable to the MV bands for the other compounds. The **Hy**-to-**Hy**$^+$ superexchange band should occur near 14 000 cm^{-1} in AN for this compound.[31]

measure accurately, are less regular but all in the predicted direction, and tend to decrease as bridge size increases for the compounds studied (see ref 9 for a discussion of the **NA**-bridged compounds; H_{ab} is somewhat larger for the **^{14}NA**- than for the **^{26}NA**-bridged compound despite the distance increasing for the latter). When a single two-state model is used for class III compounds, as remains common in the literature, $\bar{\nu}_{max}$ is not expected to change with solvent because it is interpreted as $2H_{ab}$, and ε_{max} is not predicted to change either, because it is related to the electron-transfer distance on the diabatic surfaces, $d_{ab} = 2\mu_{12}/4.8032$, where μ_{12} is the transition dipole moment of the band in Debye units and d_{ab} is in angstroms, as pointed out by Cave and Newton in their generalized Mulliken−Hush (GMH) theory.[32,33] However, as mentioned in the Introduction, a single two-state model does not apply to the lowest energy absorption band for the class III systems discussed here,[14,26,27] as will be discussed below.

Table 3 shows the same data as Table 2 for the **HyAr**-centered compounds studied in this work. Both $\bar{\nu}_{max}$ (the lowest energy absorption band transition energy) and ε_{max} are less sensitive to changing solvent from dichloromethane to acetonitrile for **(HyPh)$_2$PH**$^+$ than for any other case, and the $\Delta\bar{\nu}_{max}$ ratio is significantly less than 1 in both solvents. This is consistent with **(HyPh)$_2$PH**$^+$ being delocalized in both MC and AN. We note that its $\Delta\nu_{max}$ value is about 8 times the size of that for the **Me$_2$N**-centered compound, consistent with a noticeable increase in $\Delta\nu_{max}$ as H_{ab}/λ increases occurring before charge localization occurs. $\Delta\bar{\nu}_{max}$ for **(HyAn)$_2$PH**$^+$ has only a slightly larger $\Delta\bar{\nu}_{max}$ difference between AN and MC than does the **HyPh**-centered system, although its $\Delta\varepsilon_{max}$ value is almost 4 times as large. Nevertheless, its $\Delta\bar{\nu}_{max}$ ratio is still significantly less than 1 in both solvents, and consistent with it also being delocalized in both solvents. The **^{26}NA**-bridged compound has a small $\Delta\bar{\nu}_{1/2}$ ratio in MC, consistent with it being delocalized. Although its $\Delta\bar{\nu}_{1/2}$ ratio is under 0.9 in AN, it is not as clear that it is delocalized in this higher λ solvent because its $\Delta\varepsilon_{max}$ difference is so large, over 5 times as large as for **(HyAn)$_2$PH**$^+$. Large $\Delta\varepsilon_{max}$ differences are often observed when a delocalized compound is compared to a localized one.[19−21] Nevertheless, both because the transitions for class II and class III compounds are not closely related and because ε_{max} is harder to measure accurately than band positions and widths because of decomposition, we suggest that caution should be used in interpreting $\Delta\varepsilon_{max}$ differences. Although **(HyPh)$_2$^{14}NA**$^+$ has a smaller number of bonds between the hydrazine units than its 2,6-substituted analogue, it appears to be closer to the borderline by the criterion of $\Delta\bar{\nu}_{1/2}$ ratio, which is greater than 1 in AN, suggesting that it might be localized in AN. Although analysis of the optical spectrum of **(HytBu)$_2$^{14}NA**$^+$ gave a slightly larger H_{ab} (1510 cm^{-1} in MeCN) than did that of **(HytBu)$_2$^{26}NA**$^+$ (1410 in cm^{-1} MC and 1300 cm^{-1} in acetone), the twist at the Ar−N bonds is expected to be significantly larger for the **HytBu** than the **HyPh** CBUs. The B3LYP/6-31G* calculations gave C−N twist angles of 13° for the 2,6-isomer and 38−39° for the 1,4-isomer, which has an ortho benzo substituent at each C−N bond. H_{ab} should be approximately proportional to the product of the cosines of these angles at each C−N bond, so a turnaround of which substitution pattern produces the larger H_{ab}/λ ratio could easily occur. The **AN** bridge causes even more twisting of the hydrazine unit by having two substituents ortho to it, combined with greater ease of oxidation than the other bridges.[31] This leads to special behavior for the **M = HytBu** radical cation, with the lowest energy band not corresponding to the **M**-to-**M** superexchange that Hush theory treats but to anthracene to **Hy**$^+$ electron transfer, and anomalously fast electron transfer as a result. The similarity in spectra for the **HytBu**-centered and **HyPh**-centered cases (see Figure 5) leads us to also assign the lowest energy band for it as a bridge-to-**Hy**$^+$ electron-transfer band, so even if it were localized, like the **HytBu**-centered case was shown to be by ESR, the MV band to which Hush theory refers would be obscured by this band. B3LYP/6-31G* calculations gave C−N twists of 46 and 48° for **(HyPh)$_2$AN**$^+$. The lowest energy band $\bar{\nu}_{max}$ is even less sensitive to solvent change than the **PH**-bridged example, but the ε_{max} increase is uncertain because compound decomposition was a problem; since the absorption in this region at least in part does not correspond to the MV band, this parameter would not be significant anyway. Decomposition was also reported for **(An$_2$N)$_2$AN**$^+$.[21] **(HyPh)$_2$BI**$^+$ is unquestionably charge-

TABLE 3: Comparison of Optical Spectra for $(HyPh)_2B^+$ MV Compounds ($\bar{\nu}_{max}$, $\Delta\bar{\nu}_{1/2}$, and $\Delta\bar{\nu}_{max}$ Are in Units of 10^3 cm^{-1}, and ε_{max} Is in Units of 10^3 M^{-1} cm^{-1})[†]

		in CH_2Cl_2 (MC)			in MeCN (AN)				
B	n[a]	$\bar{\nu}_{max}$ (ε_{max})	$\Delta\bar{\nu}_{1/2}$	$\Delta\bar{\nu}_{1/2}$ ratio[b]	$\bar{\nu}_{max}$ (ε_{max})	$\Delta\bar{\nu}_{1/2}$	$\Delta\bar{\nu}_{1/2}$ ratio[b]	$\Delta\bar{\nu}_{max}$[c]	$\Delta\varepsilon_{max}$[d]
PH	5	10.70 (12.24)	3.52	**0.71**	11.10 (11.92)	3.61	**0.71**	0.40	0.32
PH[e]	5	10.07 (11.16)	3.85	**0.80**	10.57 (9.94)	4.04	**0.82**	0.50	1.22
^{26}NA	7	9.05 (15.50)	3.28	**0.72**	9.80 (9.20)	4.14	**0.87**	0.75	6.30
^{14}NA	5	9.20 (4.90)	4.24	0.92	10.40 (3.16)	5.32	1.09	1.20	1.74
AN	5	7.80 (~4.48)[f]	3.40[f]	0.77[f]	8.10 (>3.50)[f]	3.70[f]	0.93[f]	0.30[f]	<0.98[f]
BI	9	9.30 (10.50)	6.65	*1.43*[g]	12.00 (5.30)	7.00	*1.33*[g]	2.70	5.20

[†] Footnotes *a*−*d* are the same as those for Table 2. MV band $\Delta\bar{\nu}_{1/2}$ ratios under 0.9 are shown in boldface, because narrower bands than the Hush prediction is a primary criterion for assigning compounds as delocalized. [e] The charge-bearing unit is **HyAn**, not **HyPh**. [f] Assigned to bridge oxidation, as for the **HytBu**-substituted compound, so it is not a Hush-type MV band. [g] This large number is likely to indicate unresolved overlap of bridge oxidation and MV bands.

TABLE 4: Koopmans-Based B3LYP/6-31G* Calculations Class III $(HyPh)_2Ar^+$ $\bar{\nu}_{max}$ (Units of 10^3 cm^{-1}) and Comparison with Observed Band Maxima in MC

M	**B**	n	calc. $\bar{\nu}_{max}$	diff.[a] 10^3 cm^{-1}
HyPh	**PH**	5	9.62	1.08
HyPh	**^{14}NA**	7	7.61	1.59
HyPh	**^{26}NA**	5	8.05	1.00
HyPh	**AN**	5	6.89	0.91
HyPh	**BI**	9	5.82	3.48

[a] Observed $\bar{\nu}_{max}$(MC) (see Table 3) − calculated $\bar{\nu}_{max}$.

localized in AN; it shows slow electron transfer by ESR. It also shows a $\Delta\bar{\nu}_{max}$ value that is even larger than that for **$(HytBu)_2BI^+$** and a large $\Delta\varepsilon_{max}$ value. These criteria suggest that it might be delocalized (or close to it) in MC, but the $\Delta\bar{\nu}_{1/2}$ ratio is so large in both solvents that it suggests overlap of the observed low energy band with a bridge oxidation band, so it is not entirely clear whether this is the case.

We next consider calculations of the transition energy for these compounds. Koopmans-based B3LYP/6-31G* calculations using the energy gaps between the filled orbitals and the "singly occupied" molecular orbital and for class III diaminoaromatic radical cations[26] and between the "singly occupied" MO and the virtual ones for class III dinitroaromatic radical anions[13−15] have been found to correlate well with observed $\bar{\nu}_{max}$ values, although positive deviations of up to a few thousand cm^{-1} are found when configuration interaction becomes especially important, in smaller π system hydrocarbon radical cations.[34] B3LYP calculations incorrectly get almost all bishydrazine radical cations to be delocalized, even the **HytBu**-centered ones of Table 2 that have been experimentally established to be class II,[35] but we expect them to successfully predict the transition energies for class III examples. Table 4 shows such calculations for the **HyPh**-substituted compounds considered here, as an additional criterion for considering whether they are localized or delocalized. Both the **PH**- and **^{26}NA**-bridged compounds have the observed band maximum about 1000 cm^{-1} higher than the calculated one, consistent with them being class III compounds, but the **^{14}NA**-bridged one has a significantly higher difference, so as for the data of Table 3, it appears from Table 4 that this compound is closer to the II/III borderline than the **^{26}NA**-bridged one. The **AN**-bridged compound has a small diff. value, and the neutral in cation geometry highest occupied MO is delocalized and bridge-centered, while the HOMO−1 is delocalized and hydrazine-centered. We are, however, reluctant to conclude that **$(HyPh)_2AN^+$** is delocalized simply because the calculated transition energy is relatively close. Its **$(HytBu)_2AN^+$** analogue is charge-localized, and we would expect the transition energy if it were charge-localized to be similar to that observed for the lowest energy band. The very large diff. value for **$(HyPh)_2BI^+$** is nevertheless consistent with it being charge-localized even in MC, as it is known to be in AN.

Table 5 summarizes our assignments and makes comparisons to optical estimates of ET parameters assuming both class II behavior (Hush theory, H_{ab} calculated using eq 1 with the minor adjustment of refractive index corrections, and the band maximum giving λ), and class III behavior assuming that a single two-state model is applicable (generalized Mulliken−Hush theory), where the band maximum gives H_{ab} and the band intensity gives the electron-transfer distance on the diabatic surfaces, d_{ab}. As was the case for class III dinitroaromatic radical anions,[12] the d_{ab} values obtained using GMH theory are far smaller than any reasonable distance between the CBUs on the diabatic surfaces. We assume that this occurs for the reason pointed out in the Introduction: that the band analyzed is not between states of the same symmetry, so it does not represent a single two-state model, as was assumed in the derivation of the expression used to obtain d_{ab}. We emphasize this point because, if the d_{ab} values are clearly wrong, the H_{ab} values obtained using the same theory should not be reliable either. Since the H_{ab} values are large enough to correctly predict charge delocalization in most cases, and their behavior with bridge size is also as expected, it is still common in the literature to use the $H_{ab} = \bar{\nu}_{max}/2$ relationship.

Because we assign most of these compounds as class III, λ is not available for them from their optical spectra. We therefore consider here what λ might be for them. Although the class II λ has always been recognized to be the sum of solvent (λ_s) and internal vibational (λ_v) contributions, we had not appreciated until recently the implications of the mixing of wave functions that occurs as the class II/III borderline is approached. Equations 2 and 3 show solutions

$$E_1 = 0.5[\lambda(2X^2 - 2X + 1) + \Delta G^\circ] - 0.5[\{\lambda(2X - 1) - \Delta G^\circ\}^2 + 4(H_{ab})^2]^{1/2} \quad (2)$$

$$E_2 = 0.5[\lambda(2X^2 - 2X + 1) + \Delta G^\circ] + 0.5[\{\lambda(2X - 1) - \Delta G^\circ\}^2 + 4(H_{ab})^2]^{1/2} \quad (3)$$

for the ground state (E_1) and excited state (E_2) adiabatic surfaces using the two-state model with parabolic diabatic surfaces, which we believe were first explicitly published by Sutin.[36] Equation

TABLE 5: Assignment of $(HyAr)_2B^+$ to Robin−Day Class

M	B	*n*	class MC	H_{ab} (MC)[a]	$(\lambda)\{d_{ab}\}$[b] (MC)	class AN	H_{ab} (AN)[a]	$\lambda\{d_{ab}\}$[b] (AN)
HyPh	**PH**	5	III	(2.49)	(10.70)	III	(2.60)	(11.10)
				5.35	{2.3}		*5.55*	{2.3}
HyAn	**PH**	5	III	(2.41)	(10.07)	III	(2.45)	(10.57)
				5.04	{2.3}		*5.29*	{2.2}
HyPh	**^{26}NA**	7	III	(1.78)	(9.05)	III?	(1.64)	(9.80)
				4.53	{2.7}		*4.90*	{2.3}
HyPh	**^{14}NA**	5	III?	1.60	(9.20)	II?	1.57	10.40
				4.60	{1.7}		*5.20*	{1.5}
HyPh	**BI**	9	II?	1.64	9.30	II	1.40	12.00
				4.65	{3.1}		*6.00*	{2.0}

[a] The top H_{ab} entry uses Hush theory (eq 1 with the minor adjustment of including a refractive index correction, a factor of 0.89 in MC and 0.914 in AN) and is only valid if the compound is class II. The bottom entry, in italics, applies the two-state model to a class III system, $H_{ab} = \bar{\nu}_{max}/2$. [b] The λ entry is $\bar{\nu}_{max}$, which is only valid if the compound is class II. The bottom, $\{d_{ab,}$ Å$\}$, entry uses GMH theory and the Hush Gaussian band shape approximation for $\mu_{12} = 0.09584N(\varepsilon_{max}\Delta\bar{\nu}_{1/2}/\bar{\nu}_{max})^{1/2}$, also incorporating the refractive index correction *N*.

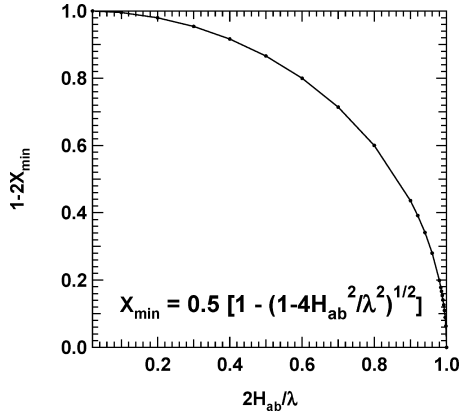

Figure 7. Plot of the ratio of the ET distance on the adiabatic to diabatic surfaces, $1 - 2X_{min}$, versus $2H_{ab}/\lambda$.

2 makes the minimum on E_1 that is closest to $X = 0$ occur at X_{min} (eq 4), and that

$$X_{min} = 0.5[1 - (1 - 4H_{ab}^2/\lambda^2)^{1/2})] \quad (4)$$

closest to 1 at $(1 - X_{min})$. The ratio of the *ET* distance on the adiabatic surfaces to that on the diabatic surfaces is therefore $(1 - 2X_{min})$. It has been traditional to consider λ_v to be a constant, but this is because Marcus and Hush only intended to use the two-state model for small H_{ab}/λ values, so that H_{ab} would cause only a perturbation to the energies. The two-state model applies at any H_{ab}/λ ratio, as pointed out by Newton and co-workers.[32,33,37] However, when a large span of $2H_{ab}/\lambda$ values is considered, one cannot consider λ_v to be a constant, because of the mixing of the wave functions of the CBUs that occurs from electronic interaction between them.[3] The mixing of the wave functions causing changes in the geometry of the CBUs is easily observed in the X-ray structure observed for **$(HytBu)_2PH^+$**.[5] At the point that $2H_{ab}$ reaches λ, the barrier to ET has entirely disappeared, because there is a single minimum and charge delocalization has occurred, so λ_v must have disappeared. Figure 7 shows a plot of the ratio of the ET distance on the adiabatic to diabatic surfaces, $1 - 2X_{min}$, versus $2H_{ab}/\lambda$, which runs from 0 at $H_{ab} = 0$ to 1 at $2H_{ab} = \lambda$. The curve is a quarter-circle. The approach of the diabatic minima as $2H_{ab}/\lambda$ is increased is initially quite slow, and the ratio only drops from 1 to 0.92 during the first 40% of the way to the II/III borderline, so λ_v is indeed effectively constant if H_{ab}/λ is small. In contrast, the drop near the II/III border is very fast, the ratio dropping from 0.436 to 0 in the last 10% of the way, as $2H_{ab}/\lambda$ goes from 0.9 to 1.0. Thus, for relatively large λ_v class II compounds like hydrazines, λ_v is the important parameter determining the ET barrier when H_{ab} is a small fraction of λ_v, but as $2H_{ab}/\lambda$ increases, λ_v is very rapidly "squeezed out" of consideration near the II/III border. Figure 7 shows that, although the CBU principally determines λ_v, it is not a constant for a given CBU but decreases as H_{ab} increases. This suggests that the size of H_{ab} necessary to cause charge delocalization will approach $\lambda_v/2$ for a given bridge, CBU combination, which might be significantly smaller than that for an isolated CBU with the bridge replaced by a hydrogen, because of electronic interaction between the CBUs.

Unfortunately, λ_v is not easy to calculate for MV compounds because calculations including electron correlation are necessary to get reasonable geometries, but B3LYP calculations, which allow cheap introduction of electron correlation, greatly overestimate the importance of electron delocalization, so they also do not get the geometry right for class II MV compounds because they delocalize nearly everything. The exchange correlation functional 50−50 (which consists of 50% Hartree−Fock + 8% Slater + 42% Becke for exchange and 19% VWN + 81% LYP for correlation)[38] has been found to localize charge and give reasonable geometric parameters for a bishydrazine radical cation lacking any aromatic substituents.[39] However, in our hands, it failed to give a reasonable geometry for the 11-bond diphenylacetylene-bridged **HyPh**-centered compound, getting only a 0.001 Å difference in N−N bond lengths at the oxidized and nonoxidized **HyPh** units. Our best estimate of what the limiting λ_v should be for aryl-substituted **HyPh**-centered compound arises from calculation of λ'_v (the enthalpy contribution to λ_v for the monohydrazine **$HyPh_2$** using the method based on the energy differences between optimized neutral, its radical cation at neutral geometry, and optimized radical cation and its neutral at radical cation geometry).[40] These calculations gave 9630 cm^{-1} using a 6-31G* basis set and 9330 cm^{-1} with a 6-31+G* basis set.[41] This procedure provides a maximum expected λ_v, which would occur when H_{ab} approached 0. These calculations suggest that an H_{ab} value of ca. 4670 cm^{-1} would be required to delocalize **HyPh**-centered MV compounds. **$(HyPh)_2{}^{14}Na^+$** appears to be rather close to the II/III border in MC, because its $\Delta\bar{\nu}_{1/2}$ value (0.92) is a little smaller than the expected value for localized compounds (1), and significantly larger than either the **PH**- or the 7-bond-bridged but less twisted **^{26}NA**-bridged radical cation. In AN, it might be localized, in which case the applicable $\lambda_v + \lambda_s$ value is 10 400 cm^{-1}, which is only 1200 cm^{-1} higher than $\bar{\nu}_{max}$ in MC, making it unlikely that both $\bar{\nu}_{max}$ values measure λ. In contrast, **$(HyPh)_2BI^+$** has a much larger $\Delta\bar{\nu}_{max}$, and both $\bar{\nu}_{max}$ values may well represent λ,

although the observed λ in MC seems uncomfortably close to the maximum value of λ_v that was calculated (9330 cm^{-1}, as mentioned above, because λ_s should be significant for a 9-bond bridge). It is not obvious how large an error is introduced by using $H_{ab} = \bar{\nu}_{max}/2$ for the class III examples. The larger value obtained for the **^{14}NA**-bridged compound than the **^{26}NA**-bridged one seems unlikely to be correct because by other criteria it appears to lie closer to the II/III borderline.

Experimental Section

2-Phenyl-d_5-2,3-diazabicyclo[2.2.2]oct-2-ene iodide (2b). Bromobenzene-d_5 (1.62 g, 10 mmol) was placed in a 250 mL flask with 25 mL of anhydrous THF. It was cooled to −78 °C, and *t*-BuLi (1.7 M in hexanes, 11.8 mL, 20 mmol) was added dropwise to give a yellow mixture. After 40 min of stirring at −78 °C, 2,3-diazabicyclo[2.2.2]oct-2-ene (1 g, 9.08 mmol) was added all at once. It was stirred for 20 min and then the dry ice bath was removed and stirring was continued for 3 h at which time it became a dark red/orange solution. It was cooled back to −78 °C, and iodine (2.79 g, 11 mmol) in 50 mL of ether was added all at once. It was stirred overnight at room temperature and was then concentrated and diluted with 150 mL of ether to precipitate a yellow/orange solid. It was recrystallized with acetonitrile and ether to give an orange solid (2.432 g, 84%). EI MS (without iodide): found, 192.1552; calcd for $C_{12}H_{10}D_5N_2$, 192.1549 (1.6 ppm). ^{1}H NMR (300 MHz, $CDCl_3$) δ 6.029−6.070 (m, 2H, NC$\underline{H}$), 2.258−2.357 (m, 4H, C$\underline{H}_2$), 1.704−1.923 (m, 4H, C$\underline{H}_2$).

2-Anisyl-2,3-diazabicyclo[2.2.2]oct-2-ene iodide (2c). To a 250 mL Schlenk flask was added 25 mL of anhydrous THF and *p*-bromoanisole (1.87 g, 10 mmol). It was cooled to −78 °C, and *t*-BuLi (1.7 M, 11.8 mL, 20 mmol) was added dropwise. After 30 min of stirring, 2,3-diazabicyclo[2.2.2]oct-2-ene (1 g, 9.08 mmol) was added all at once and the septum replaced quickly. After 1.5 h at −78 °C, the dry ice bath was removed and it was stirred at room temperature for 5.5 h. It was cooled back to −78 °C, and iodine (2.79 g, 11 mmol) in 50 mL of ether was added all at once to give a red precipitate with a dark solution. It was stirred for 2 h at room temperature and then concentrated in vacuo. Then, ether (150 mL) was added and it was filtered through a medium glass frit funnel. The deep red solid was recrystallized using acetonitrile and ether to yield deep red needles (2.73 g, 88%). ^{1}H NMR (300 MHz, $CDCl_3$) δ 8.521−8.576 (m, 2H, $C_{Ar}\underline{H}$), 7.142−7.197 (m, 2H, $C_{Ar}\underline{H}$), 6.770 (broad s, 1H, NC$\underline{H}$), 5.874 (broad s, 1H, NC$\underline{H}$), 3.973 (s, 3H, OC$\underline{H}_3$), 2.148−2.608 (m, 4H, C$\underline{H}_2$), 1.957−2.034 (m, 2H, C$\underline{H}_2$), 1.973−1.877 (m, 2H, C$\underline{H}_2$).

1,4-Bis(2-d_5-phenyl-2,3-diazabicyclo[2.2.2]oct-3-yl)-benzene-1,4-diyl-d_{10} ((HyPh)$_2$PH-d_{10}). To a 100 mL Schlenk flask was added *p*-diiodobenzene (0.310 g, 0.94 mmol) and 8 mL of anhydrous THF. After purging with nitrogen and cooling to −78 °C, *t*-BuLi was added dropwise (2.21 mL, 1.7 M in hexanes, 3.76 mmol) and it was stirred for 30 min at which time the mixture became a very thick yellow mixture. Then, 2-phenyl-d_5-2,3-diazabicyclo-[2.2.2]oct-2-ene iodide (0.6 g, 1.88 mmol) was added all at once and stirring was continued for 1 h at −78 °C. Then, the mixture was warmed to room temperature slowly over another 2 h. The mixture was stirred overnight, and the next day it was quenched with 40 mL of H_2O and 40 mL of toluene was added. The organic layer was separated and dried over Na_2SO_4 and filtered. The product was obtained (155 mg, 36%) by column chromatography with basic alumina and EtOAc/hexanes as a white solid. R_f (5% EtOAc in hexanes; alumina oxide) = 0.27. mp 246 °C (decomp). ESI MS: found, 460.3487; calcd for $C_{30}H_{24}D_{10}N_4$, 460.3487 (<1 ppm). ^{1}H NMR (500 MHz, C_6D_6) δ 6.986, 6.692 (4H, overlapping broad s, $C_{Ar}\underline{H}$), 3.657 (2H, broad s, NC$\underline{H}$), 3.625 (2H, broad s, NC$\underline{H}$), 1.927−1.845 (4H, m, C$\underline{H}_2$), 1.650−1.536 (4H, m, C$\underline{H}_2$), 1.272−1.193 (4H, broad q, C$\underline{H}_2$), 0.965−0.879 (4H, m, C$\underline{H}_2$). ^{13}C NMR[^{1}H] (125.7 MHz, C_6D_6) δ 151.43 ($\underline{C}_{Ar}$N), 144.20 ($\underline{C}_{Ar}$N), 144.16 ($\underline{C}_{Ar}$N), 115.54 ($\underline{C}_{Ar}$H), 115.45 ($\underline{C}_{Ar}$H), 48.60 (N$\underline{C}$H), 48.54 (N$\underline{C}$H), 47.99 (N$\underline{C}$H), 47.94 (N$\underline{C}$H), 25.09 ($\underline{C}H_2$), 25.06 ($\underline{C}H_2$), 24.91 ($\underline{C}H_2$), 19.76 ($\underline{C}H_2$), 19.51 ($\underline{C}H_2$), 19.42 ($\underline{C}H_2$).

1,4-Bis(2-anisyl-2,3-diazabicyclo[2.2.2]oct-3-yl)-benzene-1,4-diyl ((HyAn)$_2$PH). To a 100 mL Schlenk flask was added *p*-diiodobenzene (0.195 g, 0.59 mmol) and 7 mL of anhydrous THF. After purging with nitrogen and cooling to −78 °C, *t*-BuLi was added dropwise (1.4 mL, 1.7 M in hexanes, 2.36 mmol) and it was stirred for 35 min at which time it became a thick yellow mixture. Then, 2-anisyl-2,3-diazabicyclo[2.2.2]oct-2-ene iodide (0.41 g, 1.19 mmol) was added all at once and stirring was continued for 1.5 h at −78 °C. Then, the mixture was warmed to room temperature slowly over another 2 h. The mixture was stirred overnight, and the next day it was quenched with 40 mL of H_2O and 40 mL of toluene was added. The organic layer was separated and dried over Na_2SO_4 and filtered. The product was obtained (60 mg, 20%) by column chromatography with basic alumina and EtOAc/hexanes as a white solid. R_f (5% EtOAc in hexanes; alumina oxide) = 0.15. mp 202 °C (decomp). ESI MS: [M+H] found, 511.3060; calcd for $C_{32}H_{38}N_4O_2$, 511.3068 (1.6 ppm). ^{1}H NMR (500 MHz, C_6D_6) δ 7.095 (4H, broad s, $C_{Ar}\underline{H}$), 7.006−6.988 (4H, m, $C_{Ar}\underline{H}$), 6.816 (4H, broad t, $C_{Ar}\underline{H}$), 3.698 (2H, broad s, NC$\underline{H}$), 3.650 (2H, broad s, NC$\underline{H}$), 3.385 (6H, s, OC$\underline{H}_3$), 2.012−1.905 (4H, m, C$\underline{H}_2$), 1.745−1.673 (4H, m, C$\underline{H}_2$), 1.362−1.289 (4H, broad q, C$\underline{H}_2$), 1.030−0.972 (4H, broad q, C$\underline{H}_2$). ^{13}C NMR[^{1}H] (125.7 MHz, C_6D_6) δ 153.49 ($\underline{C}_{Ar}$O), 145.46 ($\underline{C}_{Ar}$O), 144.42 ($\underline{C}_{Ar}$N), 144.32 ($\underline{C}_{Ar}$N), 115.97 ($\underline{C}_{Ar}$H), 115.57 ($\underline{C}_{Ar}$H), 115.44 ($\underline{C}_{Ar}$H), 114.43 ($\underline{C}_{Ar}$H), 54.83 ($\underline{C}H_3$O), 48.91 (N$\underline{C}$H), 48.62 (N$\underline{C}$H), 48.44 (N$\underline{C}$H), 48.30 (N$\underline{C}$H), 25.41 ($\underline{C}H_2$), 25.16 ($\underline{C}H_2$), 19.71 ($\underline{C}H_2$), 19.63 ($\underline{C}H_2$), 19.49 ($\underline{C}H_2$).

2,6-Bis(2-d_5-phenyl-2,3-diazabicyclo[2.2.2]oct-3-yl)-napthalene-2,6-diyl-d_{10} ((HyPh)$_2$-^{26}NA-d_{10}). To a 100 mL Schlenk flask was added 2,6-dibromonapthalene (0.269 g, 0.94 mmol) and 15 mL of anhydrous THF. After purging with nitrogen and cooling to −78 °C, *t*-BuLi was added dropwise (2.21 mL, 1.7 M in hexanes, 3.76 mmol) and it was stirred for 2 h at which time the mixture became a yellow mixture. Then, 2-phenyl-d_5-2,3-diazabicyclo[2.2.2]-oct-2-ene iodide (0.6 g, 1.88 mmol) was added all at once and stirring was continued for 30 min at −78 °C. Then, the mixture was warmed to room temperature slowly over another 2 h. The mixture was stirred overnight, and the next day it was quenched by adding 40 mL of water and 40 mL of toluene. There was a thick solid still present which was present in the organic layer. The aqueous layer was removed, and the organic layer was filtered and washed with acetone to give the product as an off-white solid. This bishydrazine was not soluble to a significant degree in any organic solvents. mp 224 °C (decomp). ESI MS: [M+] calcd for $C_{34}H_{26}D_{10}N_4$, 510.3563; measuredm 510.3549 (2.7 ppm). ^{1}H NMR (300 MHz, DMSO) δ 7.51 (d, J = 8.7 Hz, 2H, $C_{Ar}\underline{H}$), 7.20 (d, overlapping with singlet, 2H, $C_{Ar}\underline{H}$), 7.17 (s, 2H, $C_{Ar}\underline{H}$), 4.29 (broad s, 2H, NC$\underline{H}$), 4.25 (broad s, 2H, NC$\underline{H}$), 2.04−1.74 (m, 8H, C$\underline{H}_2$), 1.69−1.44 (m, 8H, C$\underline{H}_2$). ^{1}H NMR (300 MHz, $CDCl_3$) δ 7.52 (broad d, 2H, $C_{Ar}\underline{H}$), 7.24 (s, overlapping with solvent, 2H, $C_{Ar}\underline{H}$), 7.19 (broad d, 2H, $C_{Ar}\underline{H}$), 4.21 (broad s, 2H, NC$\underline{H}$), 4.17 (broad s, 2H, NC$\underline{H}$), 2.24−2.04 (broad m, 4H, C$\underline{H}_2$), 1.90−1.73

(broad m, 8H, C$\underline{H}_2$), 1.58−1.46 (broad m, overlapping with water peak, 4H, C$\underline{H}_2$).

1,4-Bis(2-d_5-phenyl-2,3-diazabicyclo[2.2.2]oct-3-yl)-napthalene-1,4-diyl-d_{10} ((HyPh)$_2$-1,4NAP-d_{10}). To a 50 mL Schlenk flask was added 1,4-dibromonapthalene (0.286 g, 1 mmol) and 10 mL of anhydrous THF. After purging with nitrogen and cooling to −78 °C, *t*-BuLi was added dropwise (2.4 mL, 1.7 M in hexanes, 4 mmol) and it was stirred for 2 h at which time the mixture became a clear yellow solution. Then, 2-phenyl-d_5-2,3-diazabicyclo[2.2.2]oct-2-ene iodide (0.638 g, 2 mmol) was added all at once and stirring was continued for about 15 min at −78 °C. Then, the mixture was warmed to room temperature slowly over another 2 h. The mixture was stirred overnight, and the next day it was quenched with 40 mL of H_2O and 40 mL of toluene was added. The organic layer was separated and dried over Na_2SO_4 and filtered. The product was obtained (88 mg, 18%) by column chromatography with basic alumina and EtOAc/hexanes as a yellow solid. R_f (5% EtOAc in hexanes; alumina oxide) = 0.32. mp 227 °C (decomp). ESI MS: [M+H] found, 511.3633; calcd for $C_{34}H_{27}D_{10}N_4$, 511.3641 (1.6 ppm). ^{1}H NMR (500 MHz, C_6D_6) δ 8.580−8.538 (2H, m, C$_{Ar}\underline{H}$), 7.915 (1H, s, C$_{Ar}\underline{H}$), 7.790 (1H, s, C$_{Ar}\underline{H}$), 7.480−7.439 (2H, m, C$_{Ar}\underline{H}$), 3.813 (0.8H, broad s, NC$\underline{H}$), 3.772−3.742 (2H, m, NC$\underline{H}$), 3.546 (1.2H, broad s, NC$\underline{H}$), 2.191−1.972 (6H, m, C$\underline{H}_2$), 1.610 (1H, t, C$\underline{H}_2$), 1.439−1.329 (5H, m, C$\underline{H}_2$), 1.108−1.030 (2H, m, C$\underline{H}_2$), 0.955−0.893 (1H, m, C$\underline{H}_2$), 0.724 (1H, broad td, C$\underline{H}_2$). ^{13}C NMR[^{1}H] (125.7 MHz, C_6D_6) δ 151.62 (N$\underline{C}_{Ar}$), 151.25 (N$\underline{C}_{Ar}$), 142.69 (N$\underline{C}_{Ar}$), 142.47 (N$\underline{C}_{Ar}$), 128.77 ($\underline{C}_{Ar}$), 128.63 ($\underline{C}_{Ar}$), 125.27 ($\underline{C}_{Ar}$), 124.89 ($\underline{C}_{Ar}$H, double intensity), 124.66 ($\underline{C}_{Ar}$), 124.23 ($\underline{C}_{Ar}$H, double intensity), 117.57 ($\underline{C}_{Ar}$H, double intensity), 115.89 ($\underline{C}_{Ar}$), 53.10 (N$\underline{C}$H), 52.94 (N$\underline{C}$H), 49.52 (N$\underline{C}$H), 49.03 (N$\underline{C}$H), 25.98 ($\underline{C}H_2$), 25.90 ($\underline{C}H_2$), 25.51 ($\underline{C}H_2$), 25.38 ($\underline{C}H_2$), 20.94 ($\underline{C}H_2$), 20.84 ($\underline{C}H_2$), 20.42 ($\underline{C}H_2$), 19.83 ($\underline{C}H_2$).

9,10-Bis(2-d_5-phenyl-2,3-diazabicyclo[2.2.2]oct-3-yl)-anthracene-9,10-diyl ((HyPh)$_2$ANT). To a 50 mL Schlenk flask was added 9,10-dibromoanthracene (0.168 g, 0.5 mmol) and 6 mL of anhydrous THF. After purging with nitrogen and cooling to −78 °C, *t*-BuLi was added dropwise (1.2 mL, 1.7 M in hexanes, 2 mmol) and it was stirred for 2 h at which time the mixture became a dark brown yellow solution. Then, 2-phenyl-d_5-2,3-diazabicyclo[2.2.2]oct-2-ene iodide (0.340 g, 1 mmol) was added all at once and stirring was continued for about 15 min at −78 °C. Then, the mixture was warmed to room temperature slowly over another 2 h. The mixture was stirred overnight, and the next day it was quenched with 40 mL of H_2O and 100 mL of toluene was added (solid not very soluble in toluene). The bright red organic layer was separated and dried over Na_2SO_4 and filtered. The product was obtained by passing a toluene solution through a plug of basic alumina and eluting with EtOAc/hexanes to obtain a red solid. The red solid was then added to acetone, and it was washed several times and then filtered to give the product as a red solid (34 mg, 12%). The bright red solid was very insoluble in many common organic solvents. mp 214 °C (decomp). ESI MS: [M+] calcd for $C_{38}H_{38}N_4$, 550.3091; measured, 550.3071 (3.6 ppm). ^{1}H NMR (500 MHz, $CDCl_3$) δ 10.03−9.70 (broad s, 2H, C$_{Ar}\underline{H}$), 8.93−8.51 (broad s, 2H, C$_{Ar}\underline{H}$), 7.45−7.23 (broad s, 4H, C$_{Ar}\underline{H}$), 7.20−7.13 (m, 4H, C$_{Ar}\underline{H}$), 7.09−7.03 (m, 4H, C$_{Ar}\underline{H}$), 6.71−6.66 (m, 2H, C$_{Ar}\underline{H}$), 4.26 (s, 1H, NC$\underline{H}$), 4.20 (s, 1H, NC$\underline{H}$), 3.64 (s, 1H, NC$\underline{H}$), 3.56 (s, 1H, NC$\underline{H}$), 3.01−2.67 (broad m, 2H, C$\underline{H}_2$), 2.66−2.21 (broad m, 2H, C$\underline{H}_2$), 2.08−1.73 (broad m, 2H, C$\underline{H}_2$), 0.94−0.78 (broad m, 2H, C$\underline{H}_2$). ^{1}H NMR (500 MHz, C_6D_6, 1154 scans) δ 10.17 (broad s, 2H, C$_{Ar}\underline{H}$), 8.99 (broad s, 2H, C$_{Ar}\underline{H}$), 7.39 (broad s, 4H, C$_{Ar}\underline{H}$), ~7.23 (overlapping with solvent, 4H C$_{Ar}\underline{H}$), 6.93 (t, 4H, C$_{Ar}\underline{H}$), 6.62 (t, 1H, C$_{Ar}\underline{H}$), 6.59 (t, 1H, C$_{Ar}\underline{H}$), 3.84 (broad s, 1H, NC$\underline{H}$), 3.77 (broad s, 1H, NC$\underline{H}$), 3.52 (broad s, 1H, NC$\underline{H}$), 3.26 (broad s, 1H, NC$\underline{H}$), 2.79−0.84 (quite broad and noisy, 16H, C$\underline{H}_2$). An attempt to run a high temperature NMR (to increase the solubility) resulted in more broadening of the anthracene proton resonances.

4,4′-Bis(2-phenyl-d_5-2,3-diazabicyclo[2.2.2]oct-3-yl)-biphenyl-4,4′diyl-d_{10} ((HyPh)$_2$BIF-d_{10}). To a 50 mL Schlenk flask was added 4,4′-dibromobiphenyl (0.312 g, 1 mmol) and 10 mL of anhydrous THF. It was cooled to down to −78 °C using dry ice and acetone, and *t*-BuLi (1.7 M in hexanes, 2.4 mL, 4 mmol) was added dropwise. After stirring for 30 min at −78 °C, 2-phenyl-d_5-2,3-diazabicyclo[2.2.2]oct-2-ene iodide (0.64 g, 2 mmol) was added all at once. It was stirred for 2 h and then was allowed to warm to room temperature slowly. After 6 h of stirring at ambient temperature, it was quenched with 40 mL of water and extracted with toluene (3 × 40 mL). The organic layer was dried over $MgSO_4$, filtered and concentrated via rotovap. It was then recrystallized using toluene and acetonitrile to give 0.221 g (41%) of a white solid. mp browned 240 °C, 272 °C (decomp.) ESI MS: found, 536.3736; calcd for $C_{36}H_{28}D_{10}N_4$, 536.3724 (2.2 ppm). ^{1}H NMR (300 MHz, C_6D_6) δ 7.558 (d, J = 8.8 Hz, 4H, C$_{Ar}\underline{H}$), 7.029 (broad d, 4H, C$_{Ar}\underline{H}$), 3.690 (broad s, 4H, NC$\underline{H}$), 1.980−1.870 (m, 4H, C$\underline{H}_2$), 1.666−1.537 (m, 4H, C$\underline{H}_2$), 1.327−1.235 (m, 4H, C$\underline{H}_2$), 1.027−0.922 (m, 4H, C$\underline{H}_2$). ^{13}C NMR[1H] (75.4 MHz, C_6D_6) δ 151.35 (N$\underline{C}_{Ar}$), 150.07 (N$\underline{C}_{Ar}$), 133.22 ($\underline{C}_{Ar}$H), 115.42 ($\underline{C}_{Ar}$H), 48.68 (N$\underline{C}$H), 48.57 (N$\underline{C}$H), 25.21 ($\underline{C}H_2$), 25.19 ($\underline{C}H_2$), 20.04 ($\underline{C}H_2$), 19.98 ($\underline{C}H_2$).

Generation of the Radical Cations in Methylene Chloride and Acetonitrile. The neutral compound was dissolved in a small amount of MC (distilled over CaH_2). The silver salt used ($AgSbF_6$ or $AgPF_6$) was weighed out under a nitrogen atmosphere and added as a MC solution to the neutral compound. It was stirred for at least 20 min and then was filtered through a syringe filter (0.2 μm) into a 10.00 mL volumetric flask and diluted to the mark with MC. Then, using a volumetric pipet, a known amount (usually a 1.00 or 2.00 mL aliquot) of MC solution was transferred into a new 10.00 mL volumetric flask and several milliliters of AN were added while under nitrogen purge. The contents were purged until the volume decreased significantly, and then again AN was added. After at least 1 hour of strong purging, the solution was diluted to the mark and it was now a pure AN solution. Each solution could then be diluted further if necessary to obtain the optical concentration which was about 0.05−0.1 mM. An optical spectrum of the original MC solution was taken initially and then concurrently with the AN solution to ensure stability of the radical cation. All solutions were stable for several hours except **(HyPh)$_2$AN$^+$** in AN which decomposed. This method was carried out due to the large solvent dependence of Ag^+ and its inability to oxidize the neutral compounds directly using AN ($E°$ (MC) = 1.13V vs SCE; $E°$ (AN) = 0.42V vs SCE).

Acknowledgment. We thank NSF for support of this work under CHE-0204197 and -0647719.

References and Notes

(1) Robin, M. B.; Day, P. *Adv. Inorg. Radiochem.* **1967**, *10*, 247–422.
(2) Allen, G. C.; Hush, N. S. *Prog. Inorg. Chem.* **1967**, *8*, 357–390.
(3) Hush, N. S. *Prog. Inorg. Chem.* **1967**, *8*, 391–444.
(4) Nelsen, S. F.; Ismagilov, R. F.; Powell, D. R. *J. Am. Chem. Soc.* **1996**, *118*, 6313–6314.
(5) Nelsen, S. F.; Ismagilov, R. F.; Powell, D. R. *J. Am. Chem. Soc.* **1997**, *119*, 10213–10222.

(6) Nelsen, S. F.; Ismagilov, R. F.; Trieber, D. A., II. *Science* **1997**, *278*, 846–9.
(7) Nelsen, S. F.; Ismagilov, R. F.; Gentile, K. E.; Powell, D. R. *J. Am. Chem. Soc.* **1999**, *121*, 7108–7114.
(8) Nelsen, S. F.; Trieber, D. A. II; Ismagilov, R. F.; Teki, Y. *J. Am. Chem. Soc.* **2001**, *123*, 5684–5694.
(9) Nelsen, S. F.; Konradsson, A. E.; Teki, Y. *J. Am. Chem. Soc.* **2006**, *128*, 2902–2910.
(10) Nelsen, S. F. *Adv. Phys. Org. Chem.* **2006**, *41*, 183–215.
(11) Nelsen, S. F.; Weaver, M. N.; Luo, Y.; Pladziewicz, J. R.; Ausman, L.; Jentzsch, T. L.; O'Konneck, J. J. *J. Phys. Chem. A* **2006**, *110*, 11665–11676.
(12) Nelsen, S. F.; Konradsson, A. E.; Weaver, M. N.; Telo, J. P. *J. Am. Chem. Soc.* **2003**, *125*, 12493–12501.
(13) Nelsen, S. F.; Konradsson, A. E.; Telo, J. P. *J. Am. Chem. Soc.* **2005**, *127*, 920–925.
(14) Nelsen, S. F.; Weaver, M. N.; Telo, J. P.; Zink, J. I. *J. Am. Chem. Soc.* **2005**, *127*, 10611–10622.
(15) Nelsen, S. F.; Weaver, M. N.; Telo, J. P. *J. Am. Chem. Soc.* **2007**, *129*, 7036–7043.
(16) Nelsen, S. F.; Tran, H. Q. *J. Phys. Chem. A* **1999**, *103*, 8139–8144.
(17) Bailey, S. E.; Zink, J. I.; Nelsen, S. F. *J. Am. Chem. Soc.* **2003**, *125*, 5939–5947.
(18) Lambert, C.; Nöll, G. *Angew. Chem., Int. Ed.* **1998**, *37*, 2107–2110.
(19) Lambert, C.; Nöll, G. *J. Am. Chem. Soc.* **1999**, *121*, 8434–8442.
(20) Barlow, S.; Risko, C.; Coropceanu, V.; Tucker, N. M.; Jones, S. C.; Levi, Z.; Khrustalev, V. N.; Antipin, M. Y.; Kinnibrugh, T. L.; Timofeeva, T.; Marder, S. R.; Brédas, J.-L. *Chem. Commun.* **2005**, *76*, 4–766.
(21) Lambert, C.; Risko, C.; Coropceanu, V.; Schelter, J.; Amthor, S.; Gruhn, N. E.; Durivage, J. C.; Brédas, J.-L. *J. Am. Chem. Soc.* **2005**, *127*, 8508–8516.
(22) Barlow, S.; Risko, C.; Chung, S.-J.; Tucker, N. M.; Coropceanu, V.; Jones, S. C.; Levi, Z.; Brédas, J.-L.; Marder, S. R. *J. Am. Chem. Soc.* **2005**, *127*, 16900–16911.
(23) Szeghalmi, A. V.; Erdmann, M.; Engel, V.; Schmidt, M.; Amthor, S.; Kriegisch, V.; Nöll, G.; Stahl, R.; Lambert, C.; Leusser, D.; Stalke, D.; Zabel, M.; Popp, J. *J. Am. Chem. Soc.* **2004**, *126*, 7834–7845.
(24) Lambert, C.; Nöll, G. *J. Chem. Soc., Perkin Trans. 2* **2002**, 2039–2043.
(25) Nelsen, S. F. *Chem.—Eur. J.* **2000**, *6*, 581–588.
(26) Nelsen, S. F.; Luo, Y.; Weaver, M. N.; Lockard, J. V.; Zink, J. I. *J. Org. Chem.* **2006**, *71*, 4286–4295.
(27) Nelsen, S. F.; Weaver, M. N.; Luo, Y.; Lockard, J. V.; Zink, J. I. *Chem. Phys.* **2006**, *324*, 195–201.
(28) Sutton, J. E.; Sutton, P. M.; Taube, H. *Inorg. Chem.* **1979**, *18*, 1017–1021.
(29) D'alessandro, D. M.; Keene, F. R. *Dalton Trans.* **2004**, 3950–3954.
(30) Kaim, W.; Sarkar, B. *Coord. Chem. Rev.* **2007**, *251*, 584–594.
(31) Nelsen, S. F.; Ismagilov, R. F.; Powell, D. R. *J. Am. Chem. Soc.* **1998**, *120*, 1924–1925.
(32) Cave, R. J.; Newton, M. D. *Chem. Phys. Lett.* **1996**, *249*, 15–19.
(33) Cave, R. J.; Newton, M. D. *J. Chem. Phys.* **1997**, *106*, 9213.
(34) Nelsen, S. F.; Weaver, M N.; Bally, T.; Yamazaki, D.; Komatsu, K.; Rathore, R. *J. Phys. Chem. A* **2007**, *111*, 1667–1676.
(35) Blomgren, F.; Larsson, S.; Nelsen, S. F. *J. Comput. Chem.* **2001**, *22*, 655–664.
(36) Sutin, N. *Prog. Inorg. Chem.* **1983**, *30*, 441–499.
(37) Creutz, C.; Newton, M. D.; Sutin, N. *J. Photochem. Photobiol., A* **1994**, *82*, 47–59.
(38) Shao, Y.; Head-Gordon, M.; Krylov, A. I. *J. Chem. Phys.* **2003**, *118*, 4807–4818.
(39) Zhang, W.; Zhu, W.; Liang, W.-Z.; Zhao, Y.; Nelsen, S. F. *J. Phys. Chem. B* **2008**, *112*, 11079–11086.
(40) Nelsen, S. F.; Blackstock, S. C.; Kim, Y. *J. Am. Chem. Soc.* **1987**, *109*, 677–682.
(41) Nelsen, S. F.; Weaver, M. N.; Luo, Y.; Pladziewicz, J. R.; Ausman, L.; Jentzsch, T. L.; O'Konneck, J. J. *J. Phys. Chem. A* **2006**, *110*, 11665–11676.

JP810645Q